Meteoritics & Planetary Science 40, Nr 7, 1043–1058 (2005)
Abstract available online at http://meteoritics.org

Fine-grained, spinel-rich inclusions from the reduced CV chondrite Efremovka: II. Oxygen isotopic compositions

Jérôme ALÉON[1, 2*], Alexander N. KROT[3], Kevin D. MCKEEGAN[1], Glenn J. MACPHERSON[4], and Alexander A. ULYANOV[5]

[1]Department of Earth and Space Sciences, University of California, Los Angeles, California 90095–1567, USA
[2]Centre de Recherches Petrographiques et Geochimiques, CNRS UPR 2300, 15 rue Notre-Dame des Pauvres BP20, 54501 Vandoeuvre-les-Nancy, France
[3]Hawai'i Institute of Geophysics and Planetology, School of Ocean and Earth Science and Technology, University of Hawai'i at Manoa, Honolulu, Hawai'i 96822, USA
[4]Smithsonian Institution, Department of Mineral Sciences, NHB 119, Washington, D.C. 20560, USA
[5]M. V. Lomonosov Moscow State University, Moscow 119992, Russia
[*]Corresponding author. E-mail: aleon@crpg.cnrs-nancy.fr

(Received 23 July 2004; revision accepted 19 May 2005)

Abstract–Oxygen isotopes have been measured by ion microprobe in individual minerals (spinel, Al-Ti-diopside, melilite, and anorthite) within four relatively unaltered, fine-grained, spinel-rich Ca-Al-rich inclusions (CAIs) from the reduced CV chondrite Efremovka. Spinel is uniformly ^{16}O-rich ($\Delta^{17}O \leq -20‰$) in all four CAIs; Al-Ti-diopside is similarly ^{16}O-rich in all but one CAI, where it has smaller ^{16}O excesses ($-15‰ \leq \Delta^{17}O \leq -10‰$). Anorthite and melilite vary widely in composition from ^{16}O-rich to ^{16}O-poor ($-22‰ \leq \Delta^{17}O \leq -5‰$). Two of the CAIs are known to have group II volatility-fractionated rare-earth-element patterns, which is typical of this variety of CAI and which suggests formation by condensation. The association of such trace element patterns with ^{16}O-enrichment in these CAIs suggests that they formed by gas-solid condensation from an ^{16}O-rich gas. They subsequently experienced thermal processing in an ^{16}O-poor reservoir, resulting in partial oxygen isotope exchange. Within each inclusion, oxygen isotope variations from mineral to mineral are consistent with solid-state oxygen self-diffusion at the grain-to-grain scale, but such a model is not consistent with isotopic variations at a larger scale in two of the CAIs. The spatial association of ^{16}O depletions with both elevated Fe contents in spinel and the presence of nepheline suggests that late-stage iron-alkali metasomatism played some role in modifying the isotopic patterns in some CAIs. One of the CAIs is a compound object consisting of a coarse-grained, melilite-rich (type A) lithology joined to a fine-grained, spinel-rich one. Melilite and anorthite in the fine-grained portion are mainly ^{16}O-rich, whereas melilite in the type A portion ranges from ^{16}O-rich to ^{16}O-poor, suggesting that oxygen isotope exchange predated the joining together of the two parts and that both ^{16}O-rich and ^{16}O-poor gaseous reservoirs existed simultaneously in the early solar nebula.

INTRODUCTION

Primary minerals in Ca-Al-rich inclusions (CAIs) and amoeboid olivine aggregates (AOAs) from different chondrite groups are commonly enriched in ^{16}O by ~4–5% relative to terrestrial materials (e.g., Clayton et al. 1977; Clayton 1993; McKeegan and Leshin 2001; Yurimoto et al. 1998; Hiyagon and Hashimoto 1999; Guan et al. 2000; Fagan et al. 2001; Wasson et al. 2001; Krot et al. 2001; Aléon et al. 2002). Several hypotheses have been proposed for the origin of such ^{16}O excesses, including: 1) preservation of a nucleosynthetic anomaly carried into the infant solar system by presolar grains and subsequently incorporated into CAIs and AOAs (Clayton et al. 1977; Scott and Krot 2001), 2) mass-independent gas-phase chemistry involving asymmetric molecules in the solar nebula (Thiemens and Heidenreich 1983; Robert 2003; Marcus 2004), and 3) self-shielding in the solar nebula (Clayton 2002; Lyons and Young 2005) or in the protosolar molecular cloud (Yurimoto and Kuramoto 2004).

A parallel issue is that the CAIs in some chondrites, and particularly those in CVs, show evidence for oxygen isotopic exchange with an ^{16}O-poor reservoir that resulted in very

large degrees of isotopic heterogeneity within individual CAIs (e.g., Clayton et al. 1977). The nature of the exchange process is vigorously debated. Postulated models include: 1) diffusion-controlled post-solidification exchange of crystals with the gas reservoir, where differing diffusion rates control the degree of isotopic exchange, 2) diffusion-controlled isotope exchange during equilibrium or disequilibrium melting followed by dynamic crystallization, during which the crystallization sequence records the gradual isotopic exchange of the residual melt with the gas, and 3) post-accretion exchange between CAI minerals and aqueous fluids on the parent body.

A specific variety of refractory inclusions exists in CV chondrites—fine-grained, spinel-rich CAIs (hereafter referred to as FG-CAIs)—that can potentially provide important constraints on both the origin of the oxygen isotope anomaly and the nature of oxygen isotope exchange in CV CAIs. This is because their bulk trace element chemistry can only be explained by condensation and also because their textures and structure rule out the possibility that they experienced melting. FG-CAIs were first described in detail in the oxidized CV Allende (Wark and Lovering 1977) and later in the reduced CV chondrites Efremovka and Leoville (e.g., Ulyanov 1984; Krot et al. 2004). They are irregularly shaped aggregates that show an overall concentric structure that is defined by visual color and mineralogic variation. Their essential components are numerous, tiny (~10–20 μm in size), layered (onion-like) nodules. In Allende, those nodules consist of spinel ± perovskite ± hibonite cores surrounded by successive layers of feldspathoids, Al-diopside, and iron-rich silicates such as andradite and hedenbergite (Wark and Lovering 1977). In Efremovka and Leoville FG-CAIs, feldspathoids and iron-rich silicates are mostly absent, and the nodules consist of spinel ± perovskite ± hibonite cores surrounded by successive layers of melilite, anorthite, and Al-diopside (Ulyanov 1984; Wark et al. 1986; MacPherson et al. 2002; Krot et al. 2004). The differences between FG-CAIs in Allende and those in Efremovka and Leoville reflect the extensive iron-alkali metasomatic alteration experienced by Allende inclusions, during which anorthite and melilite were replaced by nepheline and sodalite, some perovskite was replaced by ilmenite, spinel was enriched in FeO, and calcium-iron-rich silicates were formed (e.g., Wark 1981; McGuire and Hashimoto 1989). In contrast, FG-CAIs in Efremovka and Leoville largely escaped this alteration and contain very minor nepheline and sodalite (MacPherson et al. 2002; Krot et al. 2004). Based on detailed mineralogic and petrographic studies and a thermodynamic analysis of these relatively pristine FG-CAIs, Krot et al. (2004) concluded that FG-CAIs are aggregates of gas-solid nebula condensates that experienced some thermal reprocessing but escaped significant melting. However, the most compelling evidence for a condensation origin of FG-CAIs in CV chondrites is that most of them share distinctive, volatility-fractionated group II rare earth element (REE) patterns (Tanaka and Masuda 1973; Grossman and Ganapathy 1976) that can only be explained by fractional condensation from a gaseous reservoir (Boynton 1975; Grossman and Ganapathy 1976; Davis and Grossman 1979). Therefore, oxygen isotopic compositions of these condensate CAIs can potentially provide a significant constraint on the nature of the solar nebula reservoir in which the ^{16}O-rich signature resided.

The vast majority of CAI oxygen isotope data, whether obtained on mineral separates or in situ by ion microprobe or UV laser fluorination, are for coarse-grained, igneous inclusions (CG-CAIs). Due to the high porosity and the relatively large surface areas of mineral grains in FG-CAIs, these CAIs should be more susceptible to both gas-solid oxygen isotope exchange in the nebula and oxygen isotope exchange associated with fluid-assisted thermal metamorphism in an asteroidal setting. Therefore, FG-CAIs can potentially provide an opportunity for better understanding of the relative importance of parent-body versus nebular locales for oxygen isotopic exchange. Here, we report ion microprobe measurements of oxygen isotopic compositions of four Efremovka FG-CAIs that have been recently characterized by Krot et al. (2004).

ANALYTICAL METHODS

Polished thin sections of the Efremovka FG-CAIs E42, E49-a, E67-1, and E103a were studied using backscattered electron (BSE) imaging with a JEOL JSM 5900LV scanning electron microscope. X-ray elemental mapping and electron probe microanalysis were performed with a Cameca SX-50 electron microprobe (for details, see Krot et al. 2004).

Oxygen isotopes were measured with the UCLA Cameca IMS 1270 ion microprobe in multicollection mode using a primary Cs^+ beam of ~10 μm and ~0.5 nA (Aléon et al. 2002). Oxygen isotope analyses were corrected for dead times and drifts during the course of the analyses of the respective electron multipliers by bracketing each sample with series of standard measurements. Because the ion probe beam spot (~10 μm diameter) was comparable to the size of most minerals in the FG-CAIs, many ion probe analyses sample multiple phases. Accordingly, BSE images of the ion microprobe sputter pits were processed using image processing software (Visilog 5.1) to obtain the area fractions (accurate to within ~10%) of the phases present in each analysis spot; these are reported in Table 1. Oxygen isotopic compositions in Table 1 are reported as differences in parts per thousand (per mil: ‰) from that of standard mean ocean water (SMOW): $\delta^{17,\,18}O = ([^{17,18}O/^{16}O]_{sample}/[^{17,18}O/^{16}O]_{SMOW} - 1) \times 1000$. The average analytical precisions (2σ) are ~0.4‰ and ~1.1‰ for $\delta^{18}O$ and $\delta^{17}O$, respectively. Errors listed in Table 1 take into account both the analytical precision and the semi-axis of a typical error ellipse drawn from the reproducibility on the standards (San Carlos

Table 1. Oxygen isotopic composition of fine-grained, spinel-rich CAIs in Efremovka.

Spot #	Location	Mineralogy	$\delta^{18}O$ (‰)	2σ (‰)	$\delta^{17}O$ (‰)	2σ (‰)	$\Delta^{17}O$ (‰)	2σ (‰)
E103a								
5	Core	an50 px40 sp10	–32.7	0.6	–37.0	1.7	–20.0	1.1
6	Core	an50 px30 sp20	–39.4	0.5	–40.4	2.0	–19.9	1.6
7	Core	an60 sp20 pv10 px10	–38.6	0.5	–41.5	1.7	–21.4	1.1
8	Core	an50 px30 sp20	–29.9	0.5	–33.4	1.8	–17.8	1.3
1	Mantle	mel90 sp10	–2.7	0.5	–8.2	1.7	–6.7	1.2
4	Mantle	mel90 (sp+px)10	–10.6	0.6	–16.5	1.9	–11.0	1.4
2	Mantle	mel50 sp40 hib5 px5	–13.7	0.7	–19.7	2.1	–12.6	1.7
3	Mantle	mel60 sp40 pxtr	–20.7	0.6	–25.3	1.9	–14.6	1.5
E42								
3	Core	an80 sp10 px10	–35.0	0.4	–40.6	1.7	–22.4	1.1
4	Core	an60 px30 sp10	–15.7	0.5	–18.5	1.6	–10.4	1.1
1	Mantle	mel80 an20	–40.8	0.5	–47.6	1.7	–26.4	1.2
2	Mantle	px90 an10	–38.3	0.5	–44.4	1.6	–24.5	0.9
8	Mantle	px80 an20	–25.0	0.4	–31.6	1.6	–18.6	1.0
6	Mantle	px60 an40	–29.2	0.4	–33.6	1.7	–18.5	1.2
7	Mantle	mel95 sp5	–9.3	0.5	–16.1	1.6	–11.2	1.0
5	Mantle	mel80 sp10 px10	–13.3	0.6	–15.3	1.8	–8.4	1.3
E67-1								
5	Core	an70 px20 sp10	–33.5	0.5	–36.4	1.6	–19.0	1.0
6	Core	an70 px25 sp5	–15.7	0.5	–19.4	1.6	–11.2	1.0
7	Core	an70 px20 sp10	–22.2	0.7	–25.2	1.6	–13.6	1.0
1	Mel mantle	mel60 px20 an20	–21.1	0.6	–24.3	1.7	–13.3	1.2
2	Mel mantle	mel60 px20 an20	–23.1	0.4	–27.1	1.6	–15.0	1.1
8	Mel mantle	mel60 px40	–17.0	0.5	–20.8	1.9	–11.9	1.4
9	Mel mantle	mel95 sp5	–22.6	0.5	–27.7	1.6	–16.0	1.0
3	Px mantle	px60 an40	–20.4	0.5	–21.4	1.6	–10.8	1.0
4	Px mantle	px60 an40	–21.1	0.5	–24.2	1.7	–13.2	1.2
10	Sp rim	sp80 mel10 an10	–43.0	0.4	–43.0	1.7	–20.7	1.1
E49-a								
27	FG-core	sp50 px30 an20	–35.4	0.5	–38.0	1.8	–19.5	1.3
28	FG-core	sp20 px40 an40	–23.0	0.6	–23.8	1.6	–11.9	1.1
29	FG-core	sp70 px20 an10	–38.9	0.5	–40.9	1.7	–20.6	1.2
30	FG-core	sp50 px25 an25	–34.6	0.5	–35.6	1.8	–17.6	1.3
31	FG-core	sp70 px20 an10	–36.4	0.5	–38.6	1.9	–19.7	1.4
3	FG-mantle	mel60 px30 sp10	–29.6	0.5	–31.4	1.7	–16.0	1.1
4	FG-mantle	mel95 sp5	–35.2	0.5	–38.9	1.7	–20.6	1.1
5	FG-mantle	px100	–33.4	0.5	–36.3	1.8	–18.9	1.3
6	FG-mantle	mel95 sp5	–39.4	0.5	–42.3	1.9	–21.9	1.4
7	FG-mantle	mel100	–33.2	0.6	–34.8	1.8	–17.6	1.3
8	FG-mantle	mel80 sp10 px10	–33.1	0.5	–38.0	1.8	–20.8	1.3
20	FG-mantle	px95 an5	–32.0	0.6	–38.7	2.1	–22.1	1.7
21	FG-mantle	mel100	–0.4	0.6	–4.4	1.8	–4.2	1.4
22	FG-mantle	mel95 sp5	–37.6	0.6	–40.9	2.0	–21.4	1.6
23	FG-mantle	px95 (sp+an)5	–31.8	0.5	–35.0	1.8	–18.4	1.3
24	FG-mantle	mel100	–27.9	0.5	–31.0	1.6	–16.5	1.1
1	TA	mel95 sp5	–3.7	0.5	–10.9	1.7	–8.9	1.1
2	TA	px100	–32.7	0.5	–38.3	1.6	–21.3	1.0
9	TA	mel100	–37.3	0.6	–38.2	1.6	–18.8	1.0
10	TA	mel95 sp5	–16.5	0.5	–21.6	1.6	–13.0	1.0
11	TA	mel100	4.1	0.6	–3.6	1.7	–5.8	1.1
12	TA	mel100	–6.4	0.5	–11.1	1.8	–7.7	1.3
13	TA	mel100	5.9	0.5	–2.3	1.9	–5.3	1.4
14	TA	mel90 pv5 px5	–12.5	0.5	–22.5	1.7	–16.0	1.1
15	TA	mel95 sp5	–30.1	0.5	–37.5	2.2	–21.8	1.8

Table 1. *Continued.* Oxygen isotopic composition of fine-grained, spinel-rich CAIs in Efremovka.

Spot #	Location	Mineralogy	$\delta^{18}O$ (‰)	2σ (‰)	$\delta^{17}O$ (‰)	2σ (‰)	$\Delta^{17}O$ (‰)	2σ (‰)
16	TA	mel100	−11.4	0.6	−16.2	1.8	−10.3	1.3
17	TA	mel95 sp5	−10.8	0.5	−16.5	2.0	−10.9	1.6
18	TA	sp100	−43.1	0.5	−43.3	1.8	−20.8	1.3
19	TA	px95 pv5	−36.3	0.6	−40.3	1.6	−21.4	1.0
25	TA	mel100	−37.5	0.6	−39.0	1.6	−19.5	1.1
26	TA	mel90 sp10	−37.4	0.5	−40.2	2.0	−20.8	1.6

an = anorthite; hib = hibonite; mel = melilite; px = Al-Ti-diopside; pv = perovskite sp = spinel; FG = fine-grained; TA = type A.

olivine, 77-228 olivine and Burma spinel). ^{16}O excesses are reported as the deviations in ^{17}O from the terrestrial mass fractionation line: $\Delta^{17}O = \delta^{17}O - 0.52 \times \delta^{18}O$.

RESULTS

Mineralogy and Petrology

The mineralogy, petrology, and bulk chemical compositions of the Efremovka FG-CAIs E103a, E42, E67-1, and E49-a are described in detail by Krot et al. (2004). Only a brief description is given here as a reference for the oxygen isotope discussion.

E103a is an irregularly shaped, elongated inclusion, ~1 × 3.5 mm in size (Fig. 1). It is mineralogically zoned with a spinel-anorthite-rich core and a spinel-melilite-rich mantle. The core consists of layered nodules, ~10–20 μm in apparent diameter, each composed of spinel + hibonite ± perovskite core surrounded by thin layers of melilite, anorthite, and Al-diopside. In the inclusion mantle, the melilite layer around each nodule is about 3 to 5 μm thick; anorthite is absent, and the Al-diopside layer is very thin (<1–2 μm).

E42 is a convoluted CAI, ~6 mm in the largest dimension, with a spinel-anorthite-rich core and a melilite-rich mantle (Fig. 2). The core consists of irregularly shaped spinel nodules with minute perovskite grains. Each nodule is surrounded by a thick layer of anorthite and an outer thin layer of Al-Ti-diopside. The inclusion mantle is composed of melilite that locally encloses spinel and is surrounded by Al-diopside; in some places, melilite is replaced by anorthite.

E67-1 is ~2 mm in apparent diameter and has a complex concentrically zoned structure (Fig. 3). The core is dominated by spinel nodules layered in anorthite and Al-Ti-rich pyroxene, and the abundance of spinel nodules decreases and that of anorthite increases with increasing distance from the center. The mantle contains abundant melilite, but the proportion of melilite is highest in the innermost and outermost parts of the mantle and lower in an intermediate zone; this intermediate mantle zone is richer in pyroxene. The CAI is surrounded by a discontinuous, monomineralic rim of spinel. This CAI is known to possess a fractionated group II REE pattern (Huss et al. 2002).

E49-a is a compound object, consisting of a mineralogically zoned, fine-grained, spinel-rich inclusion that is attached along a somewhat linear boundary to a coarse-grained, melilite-rich inclusion (Fig. 4). The fine-grained, spinel-rich portion has a fractionated group II REE pattern and the coarse-grained, melilite-rich part has an unfractionated REE pattern (Huss et al. 2002). Note that this inclusion is different from another CAI, E49, which is present in the same section of Efremovka and is described by El Goresy and Zinner (1994).

The fine-grained CAI, hereafter called FG-E49-a, has a Ca-poor core and a Ca-rich mantle, and is surrounded by layers of spinel and Al-diopside. The core consists of irregularly shaped spinel-perovskite bodies surrounded by anorthite and Al-diopside layers. The mantle consists of irregularly shaped, compact regions of melilite ± spinel, each surrounded by a thick continuous layer of Al-diopside. The melilite is replaced by a fine-grained mixture of spinel and Al-diopside and is surrounded by a compact layer of Al-diopside.

The coarse-grained, melilite-rich inclusion is texturally and mineralogically similar to a type A inclusion and is hereafter called TA-E49-a. It consists of multiple, massive, melilite-rich bodies enclosing abundant perovskite grains and minor spinel-hibonite nodules. Melilite is replaced locally by a fine-grained mixture of Al-diopside and spinel and is rimmed by Al-diopside.

Oxygen Isotopic Compositions

Oxygen isotope data, including the calculated proportions of phases in each analyzed spot, are given in Table 1. The ellipses on the accompanying photographs (Figs. 1–4) show the exact locations of ion probe spots for each analysis. The data are represented graphically in Figs. 5–8. Due to the fine-grained nature of the Efremovka CAIs analyzed, most ion probe spots sampled several phases. We estimated oxygen isotopic compositions of melilite and anorthite in these mixed spots based on their modal mineralogy and mass balance calculations. If these mixed spots with variable oxygen isotopic compositions contained spinel and pyroxene and no pure analyses of these phases were obtained in the same CAI, we assumed that spinel and pyroxene retained their ^{16}O-rich compositions ($\Delta^{17}O$ ~−20‰) and the variations are mainly due to anorthite and melilite. The estimated ranges of oxygen isotopic compositions of melilite and anorthite are indicated in Figs. 5–8 by dashed and dotted areas, respectively.

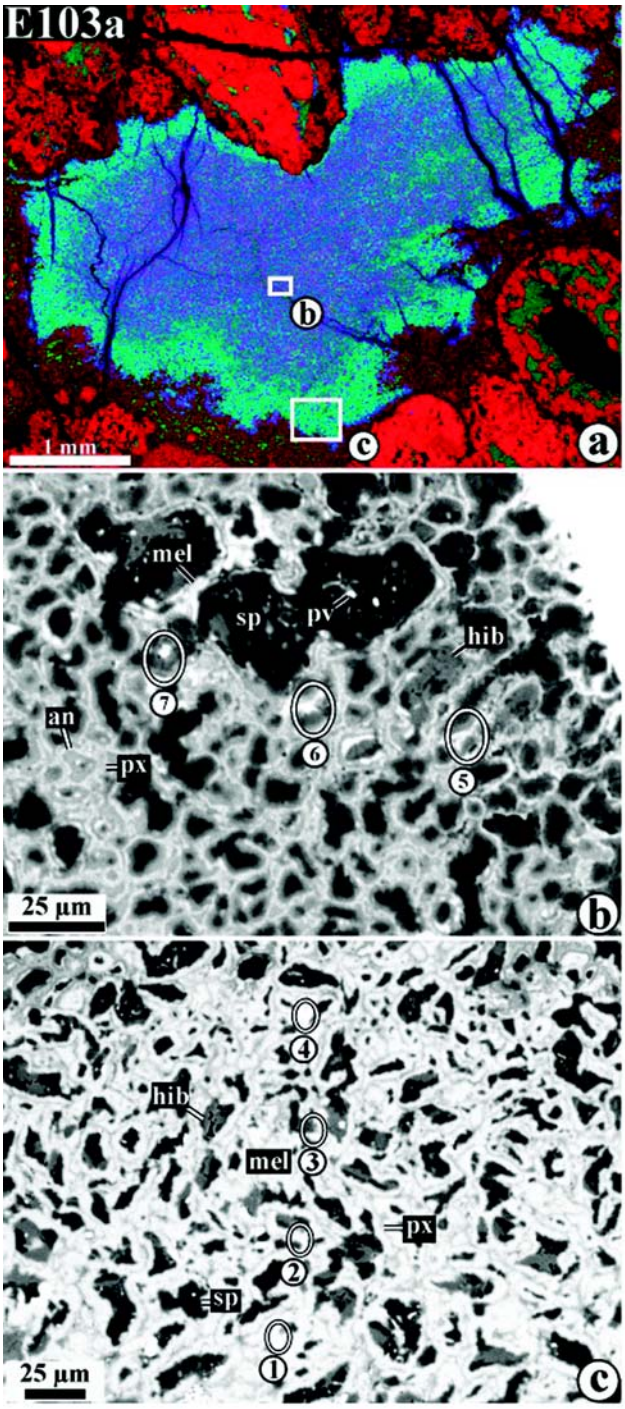

Fig. 1. Zoned, fine-grained, spinel-rich CAI E103a from Efremovka. a) Combined X-ray elemental map (Mg = red, Ca = green, Al = blue); (b, c) show BSE images of regions outlined and labeled in (a). The CAI has a melilite-poor (Ca-poor) core and a melilite-rich (Ca-rich) mantle. b) The core consists of spinel, hibonite, perovskite, anorthite, Al-diopside and minor melilite replaced by anorthite. c) The mantle is made of spinel, hibonite, melilite, perovskite and minor Al-diopside. Ellipses indicate ion probe spots; numbers correspond to ion probe analyses listed in Table 1. Abbreviations: an = anorthite; hib = hibonite; mel = melilite; px = Al-Ti-diopside; pv = perovskite; sp = spinel.

Eight analyses were collected for E103a (Fig. 1a), with four each in the spinel-rich core (Fig. 1b) and the melilite-rich mantle (Fig. 1c). Due to the very fine-grained nature of this CAI, no analyses really come close to being monomineralic. However, all compositions in the core are ^{16}O-rich (Δ^{17}O = −18‰ to −21‰) (Fig. 5), even in cases where the spots sampled significant anorthite in addition to spinel and pyroxene (Table 1). The estimated range of Δ^{17}O values of anorthite in the core is −14‰ to −18‰ (Fig. 5). In contrast, the mantle analyses are relatively ^{16}O-depleted (Δ^{17}O ~−7‰ to −15‰; Fig. 5) and in all cases sample mostly melilite; those spots (e.g., Fig. 1c, spot 3) that sampled significant spinel in addition to melilite are more ^{16}O-rich, suggesting that the spinel is ^{16}O-rich compared to melilite. The estimated range of Δ^{17}O of melilite is −5‰ to −10‰ (Fig. 5).

Eight analyses were obtained in E42: six in the melilite-rich mantle and two in the spinel-rich core. Both core analyses (Table 1; Fig. 6) sampled predominantly anorthite with greatly subordinate spinel and pyroxene (Fig. 2b, spots 3 and 4), yet one composition is ^{16}O-rich (Δ^{17}O ~−22‰) and the other is relatively ^{16}O-depleted (Δ^{17}O ~−10‰), indicating that Δ^{17}O of anorthite in the core varies over a wide range, from ~−20‰ to ~−5‰. Pyroxene in the mantle of E42 is consistently ^{16}O-rich; one nearly monomineralic analysis (Fig. 2b, spot #2) yielded Δ^{17}O ~−25‰. Conversely, melilite in the mantle is isotopically heterogeneous; one analysis of nearly pure melilite (Fig. 2c, spot 7) is ^{16}O-poor (Δ^{17}O ~−11‰), whereas another (Fig. 2b, spot 1) that also samples ~20% anorthite in addition to melilite is very ^{16}O-rich (Δ^{17}O ~−26‰). These observations indicate that there is no oxygen isotopic layering comparable with the mineralogical layering of E42; rather, this inclusion contains regions in both the core and mantle where melilite and anorthite are ^{16}O-enriched (<−20‰) and other regions in both in which the same phases are ^{16}O-depleted (>−10‰) compared to the uniformly ^{16}O-rich spinel and pyroxene (Fig. 6).

Ten analyses were obtained from E67-1: six in the melilite-rich mantle, three in the spinel-rich core, and one in the monomineralic spinel rim around the outside of the CAI. Relatively pure analyses were obtained only for melilite in the mantle (Fig. 3c, spot 1) and for spinel from the outermost rim (Fig. 3c, spot 10). Analyses of the core sampled primarily anorthite with subordinate pyroxene and spinel (Fig. 3f). The compositions vary considerably from intermediate to large enrichment in ^{16}O, with Δ^{17}O ~−11‰ to −19‰ (Table 1; Fig. 7). Melilite in the mantle has intermediate enrichment in ^{16}O, with Δ^{17}O ~−16‰ (Table 1; Fig. 7). Two mantle analyses (Fig. 3e, spots 3 and 4) that sampled mostly pyroxene and lesser amounts of anorthite have intermediate enrichment in ^{16}O, with Δ^{17}O ranging from −11‰ to −13‰. The spinel in the rim is ^{16}O-rich (Δ^{17}O ~−21‰). Overall, the data for this CAI indicate that pyroxene, anorthite, and melilite have

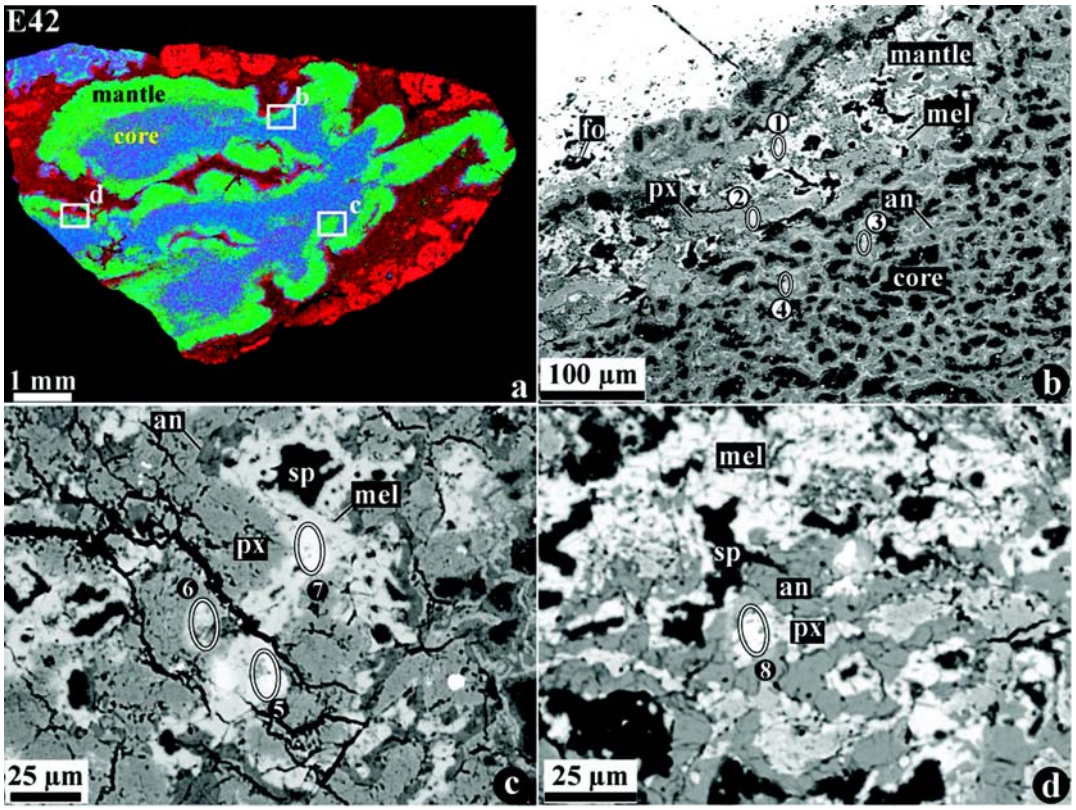

Fig. 2. Zoned, fine-grained, spinel-rich CAI E42 from Efremovka. a) Combined X-ray elemental map (Mg = red, Ca = green, Al = blue); (b–d) show BSE images of the regions outlined and labeled in (a). b) The Ca-poor core (lower right) consists of spinel, anorthite, and minor Al-diopside. (b upper left, c, d) The Ca-rich mantle is composed of Al-diopside, melilite, minor spinel, and anorthite. The CAI is surrounded by a thin forsterite-rich accretionary rim (red in [a]). Fo = forsterite; other abbreviations are as used previously. Ellipses indicate ion probe spots; numbers correspond to ion probe analyses listed in Table 1.

intermediate compositions with $\Delta^{17}O$ ranging from −17‰ to −10‰ in all petrographic layers of the inclusion; the spinel is ^{16}O-rich. Similar intermediate isotopic compositions of pyroxene, anorthite, and melilite have been reported in a FG-CAI from the reduced CV chondrite Vigarano by Fagan et al. (2004b) who used smaller ion probe spots.

A total of 31 analyses were collected from the compound inclusion E49-a, comprising 16 from the fine-grained portion FG-E49-a and 15 from the coarse-grained part TA-E49-a. Many of the analyses from both parts of the CAI sample nearly pure phases. With the exception of one melilite-rich spot in the mantle, the oxygen isotopic compositions of melilite, spinel, and pyroxene (and their mixtures) in both the core and mantle of FG-E49-a are almost uniformly ^{16}O-enriched ($\Delta^{17}O$ = −17‰ to −22‰) and plot along the carbonaceous chondrite anhydrous mineral (CCAM) line (Table 1; Fig. 8). The lone outlier is a melilite spot in the mantle (spot 21, Table 1) that has small excess of ^{16}O ($\Delta^{17}O$ = −4‰; Fig. 8). One anorthite-rich spot in the core (spot 28, Table 1) has intermediate enrichment in ^{16}O ($\Delta^{17}O$ = −12‰; Fig. 8). In contrast to the mostly ^{16}O-rich signature in FG-E49-a, many analyses of the melilite-rich spots in TA-E49-a show far less enrichment in ^{16}O. Melilite shows extreme variations in oxygen isotopic composition, $\Delta^{17}O$ ~−22‰ up to −5‰ (Table 1; Fig. 8). Spinel in a large spinel-perovskite nodule in TA-E49-a is ^{16}O-rich (Table 1, spot 18; Fig. 4j). The compositions of most melilite grains in TA-E49-a are shifted to the right of the CCAM line and relative to the phases in FG-E49-a. The maximum shifts observed, −6.9‰ in $\delta^{18}O$ and 6.5‰ in $\delta^{17}O$, are much larger than the 2σ errors (0.5‰ and 1.7‰, respectively) and, considering that the phases in FG-E49-a (collected in the same run) are not similarly shifted, it is probable that the observed shift is not an analytical artifact.

DISCUSSION

Evidence for an ^{16}O-Rich Gaseous Reservoir in the Early Solar System

All fine-grained, spinel-rich inclusions analyzed in this study bear the ^{16}O-rich signature that has been found in many CAIs from different chondrite groups. The FG-CAIs from Efremovka show similar oxygen isotopic features to those of the CG-CAIs in CV chondrites: spinel is ^{16}O-enriched ($\Delta^{17}O$ < −20‰) and other minerals have variable oxygen isotopic compositions with Al-diopside enriched in ^{16}O ($\Delta^{17}O$ from

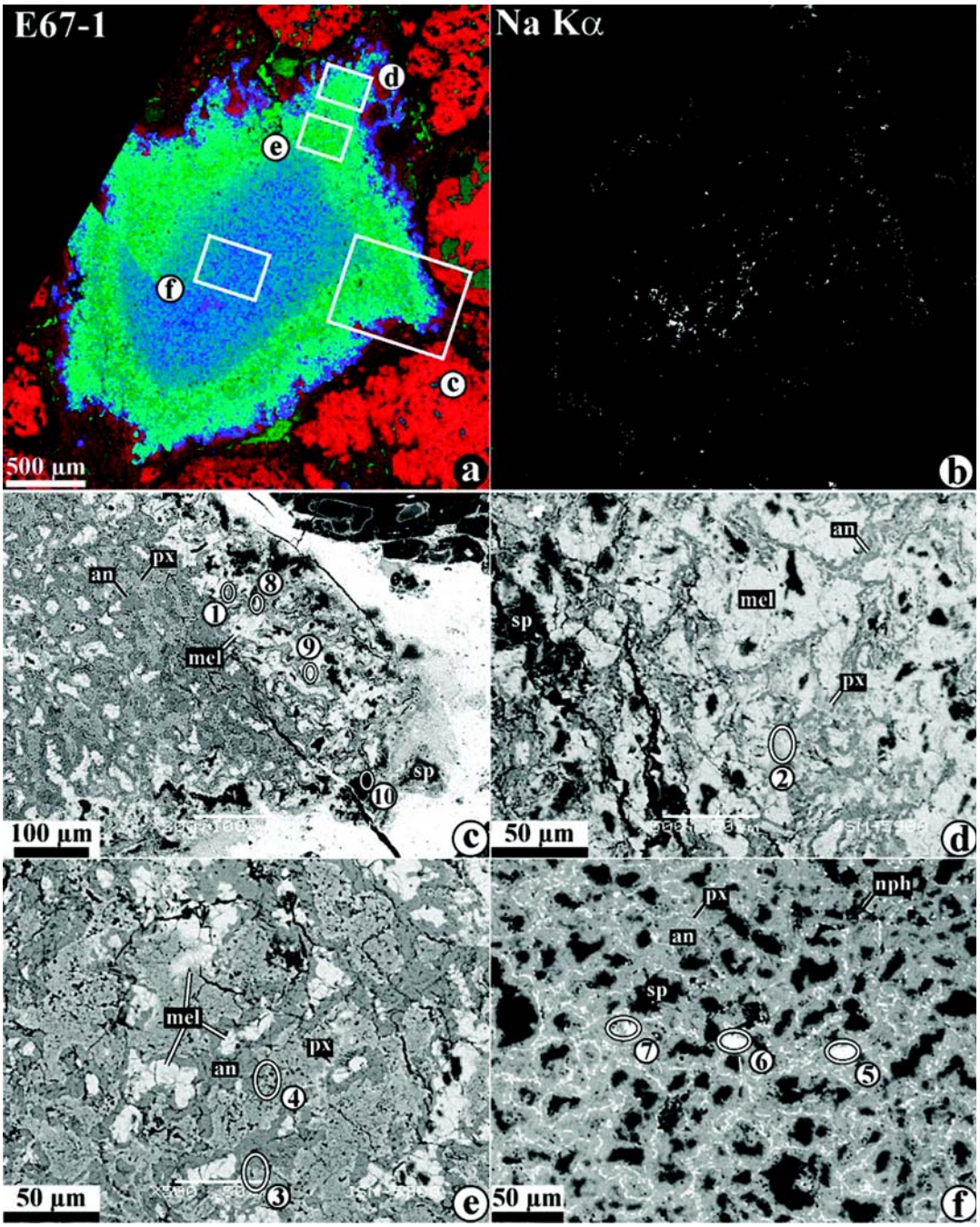

Fig. 3. Zoned, fine-grained, spinel-rich CAI E67-1 from Efremovka. a) A combined X-ray elemental map (Mg = red, Ca = green, Al = blue). b) An X-ray element area map for Na K. (c–f) show BSE images of regions outlined and labeled in (a). f) The Ca-poor core consists of spinel, anorthite, Al-diopside, and secondary nepheline. The Ca-rich mantle can be divided into the inner, pyroxene-rich zone (e) and outer, melilite-rich zone (c, d); both consist of melilite, Al-diopside, anorthite, and spinel, but in different proportions. The CAI is surrounded by a spinel-rich rim. Nph = nepheline; other abbreviations are as used previously. Ellipses indicate ion probe spots; numbers correspond to ion probe analyses listed in Table 1.

< −20‰ to −10‰) compared to melilite and anorthite ($\Delta^{17}O$ from −22‰ to −2‰). Within each inclusion, anorthite and melilite tend to be more variable in composition than either spinel or pyroxene. Based on these observations, we infer that the FG-CAIs and CG-CAIs from CV chondrites formed and evolved in the same oxygen isotopic reservoirs.

Where the fine-grained, spinel-rich CAIs differ from most other inclusion types is in their evolution history. The compositions of virtually all CAIs suggest formation by a volatility-controlled process, but only in a very few cases does the evidence point unambiguously to condensation rather than evaporation. Indeed, the relative roles of the two

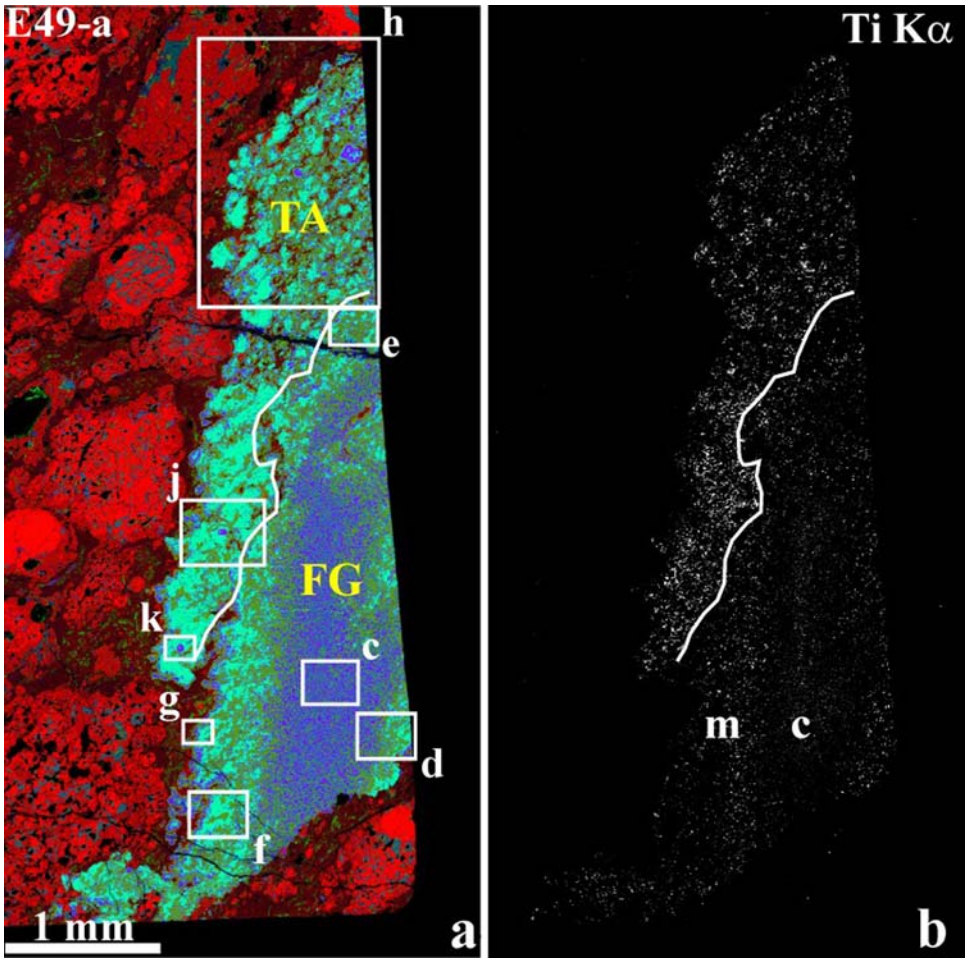

Fig. 4. The compound Efremovka CAI E49-a. a) Combined X-ray elemental map [Mg = red, Ca = green, Al = blue]; (b) X-ray element area map for Ti K; (c–k) show BSE images of regions outlined and labeled in (a). The dominant portion of the CAI is a zoned fine-grained, spinel-rich inclusion (FG); the upper left region in (a) and (b) is a coarse-grained, melilite-rich (type A, TA) inclusion. The boundary between these lithologies is indicated by a solid line. The fine-grained CAI has a well-defined core-mantle structure.

processes in CAI genesis continue to be a source of vigorous debate (e.g., Davis and Richter 2004). Additionally, most CG-CAIs show clear evidence of melting, evaporation, and/or re-crystallization, and, even if their precursors did originate by condensation, very few can remotely be described as pristine condensates. In contrast, the mineralogy, petrology, and group II REE patterns of FG-CAIs from CV chondrites indicate that these inclusions are nebular-gas condensates, although their mineralogical zoning suggests that they experienced multiple heating events (Boynton 1975; Davis and Grossman 1979; Huss et al. 2002; Krot et al. 2004). Our results demonstrate an association in these CAIs of an ^{16}O-rich signature with phases that must have formed by condensation. The oxygen isotopic composition of individual minerals in the FG-CAIs studied here show that they were initially ^{16}O-rich and subsequently re-equilibrated with an ^{16}O-poor reservoir.

Krot et al. (2002) recently suggested that some forsterite-rich coarse-grained accretionary rims around CV CAIs formed by condensation from an ^{16}O-rich gaseous reservoir, which is contrary to the long-held view that dust rather than gas was the source of the ^{16}O-rich signature that is so typical of refractory materials from the early solar system. The present work makes an even stronger case for the same conclusion because, so far as anyone has ever been able to show, the group II trace element signature that characterizes these CAIs can only result from condensation.

Implications for Oxygen Isotopic Heterogeneity within CV Chondrite CAIs

Although most CAIs from most chondrite groups share in common an original ^{16}O-rich signature, the patterns within each chondrite group differ greatly. For example, in ordinary and enstatite chondrites, most CAIs are ^{16}O-enriched and individual CAIs show little or no internal variation (McKeegan et al. 1998; Guan et al. 2000; Fagan et al. 2001); these signatures preserve intact the isotopic composition of the reservoir out of which the CAIs originally formed. In

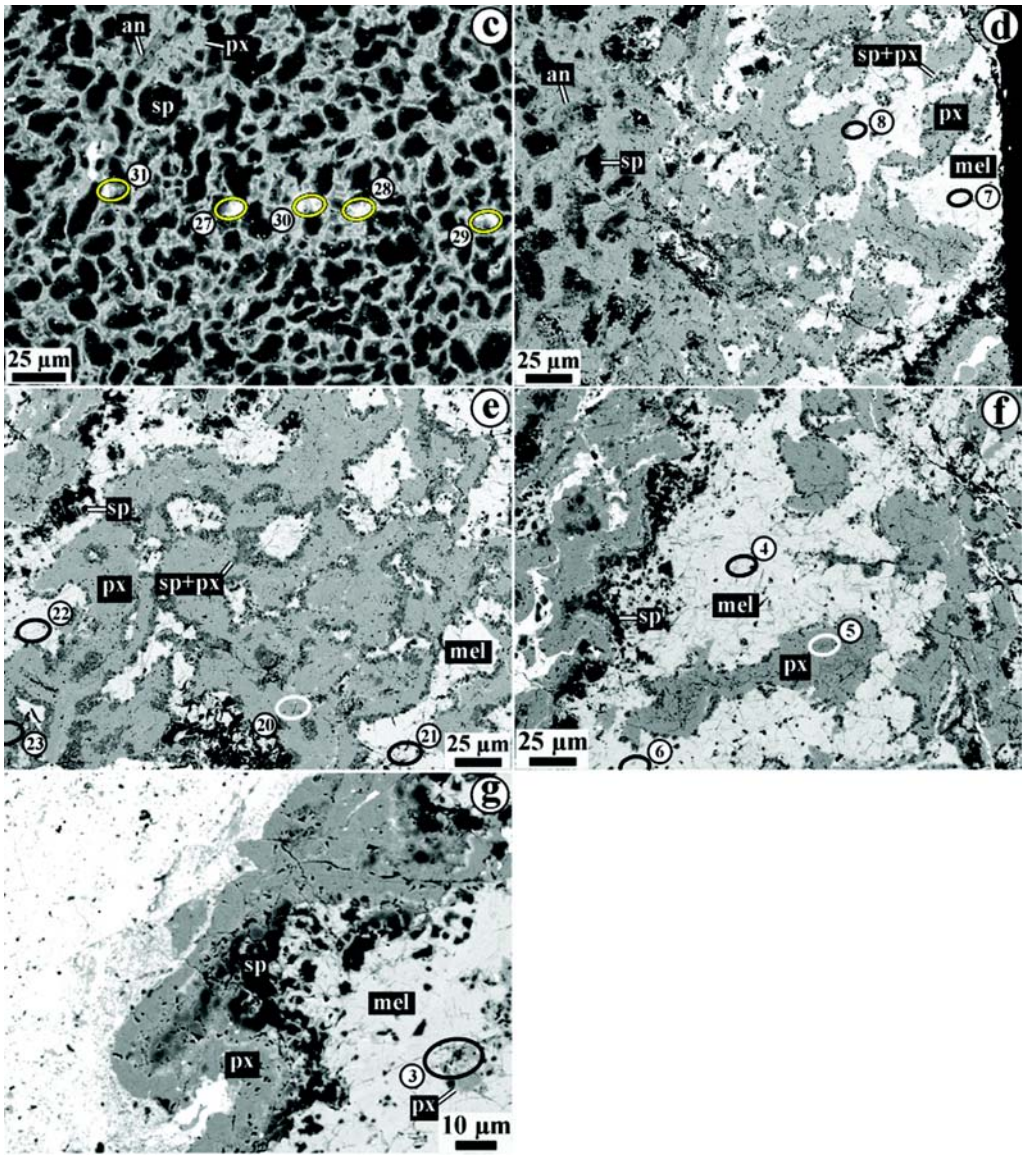

Fig. 4. *Continued.* c) The Ca-poor core consists of irregularly shaped spinel-perovskite bodies, each surrounded by an anorthite layer and a thin layer of Al-diopside. d–g) The Ca-rich mantle is composed of irregularly shaped melilite regions surrounded by coarse-grained Al-diopside. Melilite is replaced by a fine-grained mixture of Al-diopside and spinel.

contrast, all CAIs in CB carbonaceous chondrites and some—those with igneous textures—in CR, CO, and CH chondrites are ^{16}O-depleted with minimum $\Delta^{17}O \geq -10‰$ (Sahijpal et al. 1999; Krot et al. 2001; Aléon et al. 2002; Itoh et al. 2004). Such isotopic compositions are attributed to the remelting of initially ^{16}O-rich CAIs in an ^{16}O-poor gaseous reservoir (Aléon et al. 2002; Itoh et al. 2004). Different yet again are the CAIs in CO chondrites, whose oxygen isotopic compositions appear to correlate with the degree of thermal metamorphism experienced by the host meteorites (Wasson et al. 2001). In these CAIs, melilite is progressively depleted in ^{16}O with increasing metamorphic grade, and this pattern is interpreted to reflect oxygen isotopic exchange during fluid-rock interaction in an asteroidal setting (Wasson et al. 2001). Finally, CAIs in CV chondrites show very large internal oxygen isotopic heterogeneity. Most igneous CAIs (compact type A, type B and type C) have ^{16}O-rich spinel, hibonite, Al-Ti-diopside, and olivine along with ^{16}O-poor melilite and/or anorthite (e.g., Clayton et al. 1977; McKeegan and Leshin 2001). In addition, oxygen isotopic zoning has been observed in Al-Ti-diopside and melilite (Yurimoto et al. 1998; Ito et al. 2004). The origin of these heterogeneities remains poorly understood, and all of the models that have been proposed suffer from significant difficulties.

For example, the original and still most widely accepted model postulates post-crystallization, solid state isotopic exchange with a nebular gas that was ^{16}O-poor (Clayton et al. 1977). In this model, the isotopic differences between the CAI

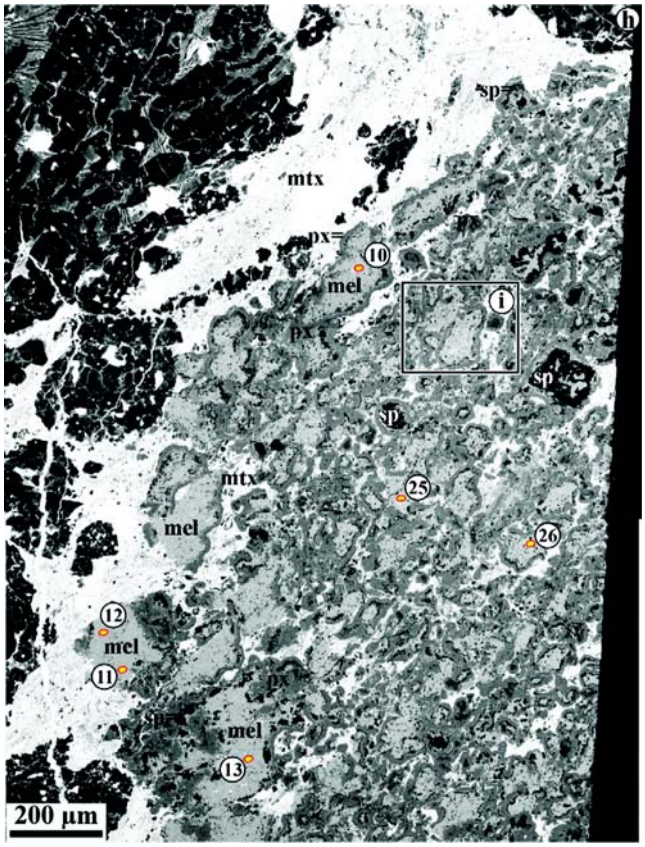

Fig. 4. *Continued.* h) Large-scale view of the type A part of the CAI which consists of multiple melilite bodies. Details are shown in Figs. 4i-k. Abbreviations as used previously. Ellipses indicate ion probe spots; numbers correspond to ion probe analyses listed in Table 1.

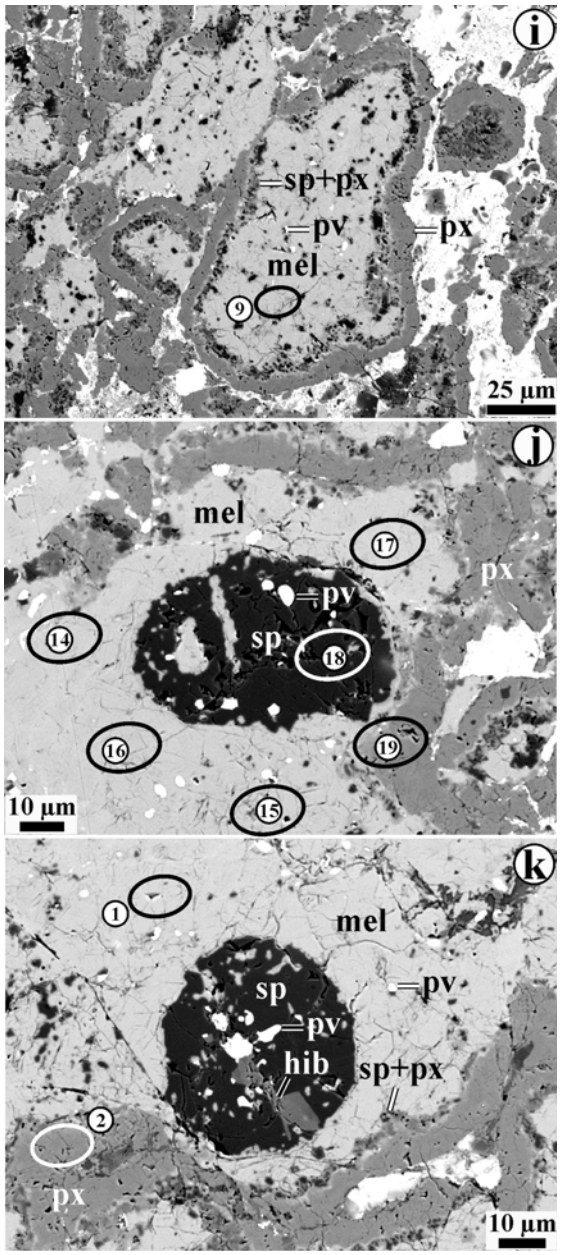

Fig. 4. *Continued.* i–k) Melilite bodies in the type A part of the CAI are full of enclosed spinel and perovskite grains and rimmed by Al-diopside. Also present in this portion of the CAI are several large spinel-perovskite-melilite ± hibonite nodules (j, k). Melilite is corroded by a fine-grained mixture of spinel and Al-diopside. Abbreviations are as used previously. Ellipses indicate ion probe spots; numbers correspond to ion probe analyses listed in Table 1.

minerals reflect differences in diffusion rate so that, for example, spinel, which has a very slow diffusion rate, retained its ^{16}O-rich signature, whereas melilite and anorthite which have much faster diffusion rates, did not. However, detailed experimental studies of oxygen self-diffusion showed that the observed relative isotopic compositions of CAI phases (especially pyroxene) are not quantitatively consistent with the diffusion rates (Yurimoto et al. 1989; Ryerson and McKeegan 1994).

The second model for the oxygen isotopic variations of CV CAIs involves partial isotopic exchange during crystallization following equilibrium melting, where the melting takes place in an ^{16}O-poor gaseous reservoir, unlike that in which the CAIs originally formed. In this model, the isotopic compositions of phases should track the order of crystallization as the residual melt equilibrates isotopically with the external gas. However, this model is inconsistent with the experimentally studied crystallization sequence of minerals in igneous CAIs such as the type B CAIs in CV chondrites (Stolper 1982). For example, melilite, which crystallizes prior to pyroxene, should therefore be consistently ^{16}O-rich relative to pyroxene, however, the opposite is observed to be true. A theoretical model of oxygen isotope exchange during disequilibrium melting recently proposed by Greenwood (2004) may explain the observed oxygen isotope patterns in coarse-grained, igneous CAIs from CV chondrites, but requires a very complex thermal history of the CV CG-CAIs and has not been tested experimentally yet.

Finally, another model postulates fluid-rock isotope exchange on the chondrite parent asteroid or asteroids. For example, Young and Russell (1998) hypothesized that this

process might have played an important role in establishing the CAI isotopic mixing line, having found evidence for a slope = 1.0 line defined by unaltered minerals (including melilite) in an Allende CAI. In this model, the shallower slope of the CCAM-mixing line (~0.94) results from isotopic exchange with an aqueous phase during mineral alteration. Although similar processes have been invoked to explain both bulk oxygen isotopic compositions of carbonaceous chondrites as well as oxygen isotopic compositions of their individual components (e.g., chondrules or matrix) and minerals (e.g., phyllosilicates, carbonates, or magnetite), no quantitative application to CAI minerals has been attempted yet (Clayton and Mayeda 1984; Young et al. 1999). Isotopic exchange by such a process depends on several variables, such as fluid temperature and isotopic and chemical composition, as well as the density of the crystal defects in CAI minerals. So far, none of these parameters have been studied experimentally in connection with fluid-assisted oxygen isotope exchange in CAIs.

Similar to coarse-grained, igneous CAIs from CVs, the FG-CAIs from Efremovka show internal oxygen isotope heterogeneity, with spinel and pyroxene enriched in ^{16}O compared to anorthite and melilite, which suggests partial equilibration with an ^{16}O-poor reservoir. Unlike CG-CAIs, however, all FG-CAIs we studied contain melilite and anorthite that range in oxygen isotopic compositions from ^{16}O-rich to ^{16}O-poor. In addition, the degree of ^{16}O-depletion of melilite and anorthite in FG-CAIs is generally smaller than those in CG-CAIs from CV chondrites (Figs. 5–8).

Based on the mineralogy, petrology and a thermodynamic analysis of FG-CAIs from the reduced CV chondrites, Krot et al. (2004) concluded that these inclusions originally formed as aggregates of spinel-perovskite-melilite ± hibonite gas-solid condensates, which subsequently experienced lower-temperature gas-solid reactions in the solar nebula, with gaseous SiO and Mg to form Al-diopside and anorthite layers around the spinel-rich nodules. Krot et al. (2004) further interpreted the overall zoned structures of the FG-CAIs to be the result of subsequent re-heating that resulted in evaporative loss of SiO and Mg and formation of melilite. This interpretation is in apparent conflict with the observation of isotopically light, rather than heavy, Mg by early studies of FG-CAIs from Allende (Esat and Taylor 1984; Brigham et al. 1985). However, those Allende objects exhibit extensive alteration and replacement of melilite by secondary minerals such as nepheline, and therefore may not be isotopically representative of their precursors. The Krot et al. (2004) model requires additional testing by high-precision magnesium isotopic measurements of mantle melilite in Efremovka and Leoville FG-CAIs.

The ^{16}O-rich compositions of most of the anorthite and pyroxene grains in the cores of 103a, E42, and E49-a, some in E67-1, and most of the melilite grains in the mantles of E42 and E49-a (Table 1) suggest that the formation of anorthite,

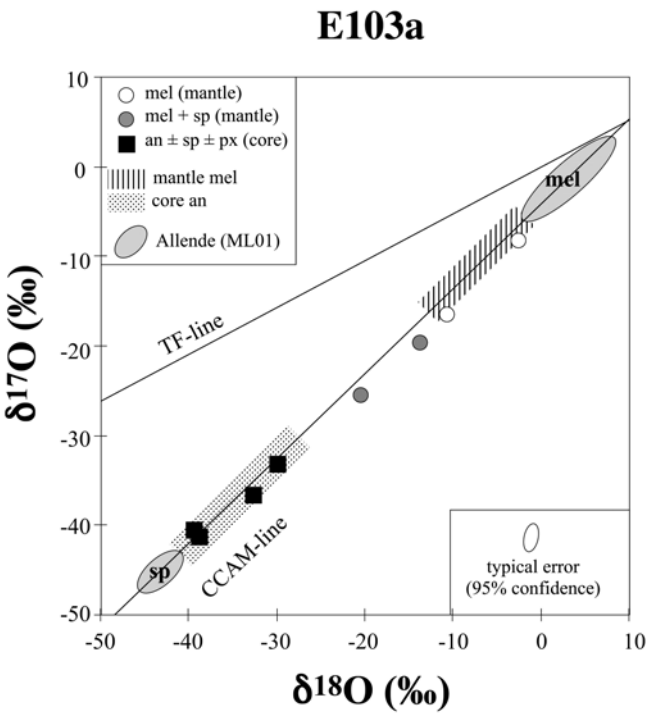

Fig. 5. Oxygen isotopic composition of the Efremovka CAI E103a. Black symbols denote measurements in the CAI core; white and grey symbols those in the CAI mantle. Terrestrial fractionation (TF) line and carbonaceous chondrite anhydrous mixing (CCAM) line are shown for reference. Here and in Figs. 6–8, dashed and dotted areas indicate the estimated range of compositions of melilite in the CAI mantle and anorthite in the CAI core (see text for details), respectively; the grey areas indicate typical compositions of spinel and melilite in coarse-grained CAIs from Allende; ML01 stands for McKeegan and Leshin (2001). Abbreviations are as used previously. The range of mantle melilite and core anorthite compositions indicates an oxygen isotope exchange limited to the mantle.

pyroxene, and melilite in the Efremovka FG-CAIs took place in an ^{16}O-rich gaseous reservoir; that is, the FG-CAIs were originally uniformly ^{16}O-enriched. The ^{16}O-poor compositions of some of the anorthite and melilite grains in E42, E67-1, and E49-a, which do not correlate with their location (core or mantle) within a host CAI, suggest that these grains experienced localized oxygen isotope exchange after formation of the overall structural zonation of the FG-CAIs. Among these CAIs, E67-1 has the highest number of analysis spots depleted in ^{16}O. It also has the highest abundance of nepheline grains (Fig. 3b), suggesting that oxygen isotope exchange in melilite and anorthite of E67-1 might indeed be linked to secondary alteration events. The exact nature and locale of such events, for example, nebular or due to localized fluid-flow on a parent-body, is not necessarily determined by these data.

In E103a, all of the melilite grains analyzed in the mantle are ^{16}O-depleted compared to the anorthite grains in the core (Table 1). This is the only CAI where the mineralogic and oxygen isotope zonations coincide. These observations can be

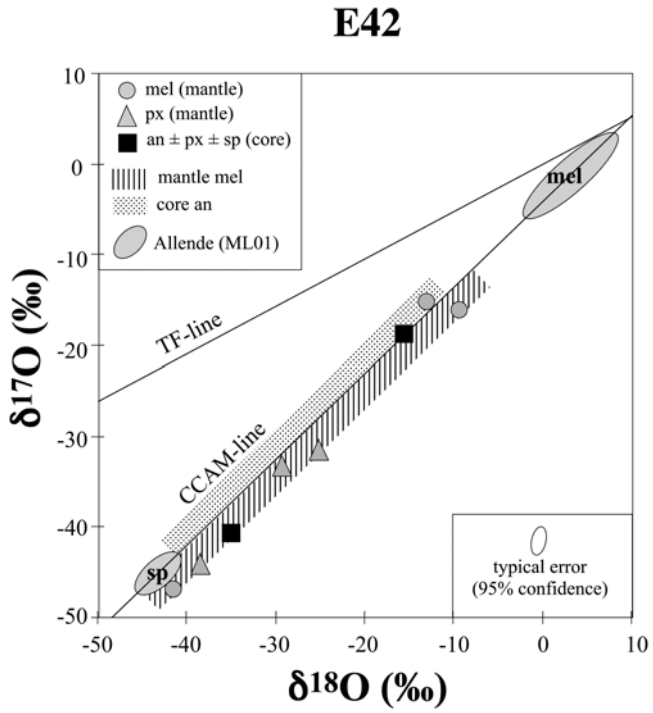

Fig. 6. Oxygen isotopic composition of the Efremovka CAI E42. Black symbols denote measurements in the CAI core; grey symbols those in the CAI mantle. Abbreviations are as used previously. The large range of compositions in both mantle melilite and core anorthite shows the heterogeneous distribution of oxygen isotope exchange in this CAI.

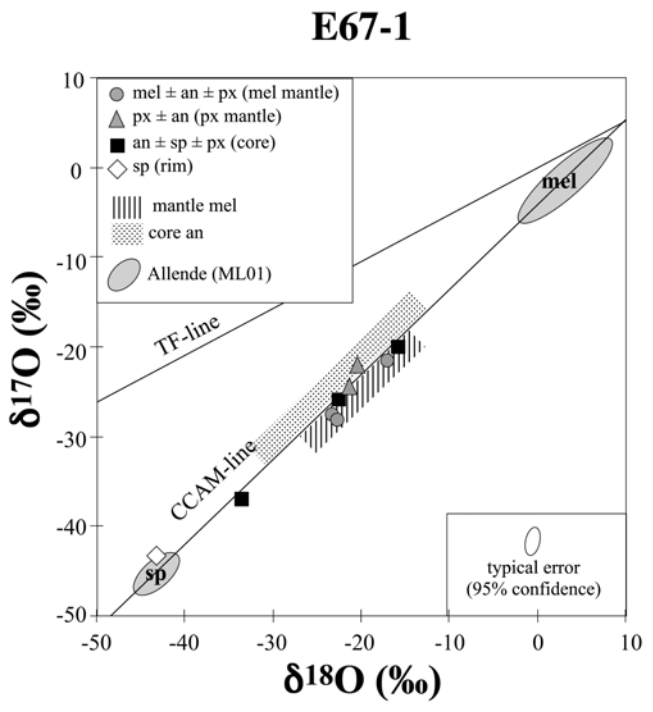

Fig. 7. Oxygen isotopic composition of the Efremovka CAI E67-1. Black symbols denote measurements in the CAI core; grey symbols those in the mantle, and white symbols those in the rim. Abbreviations are as used previously. All minerals but spinel have intermediate isotopic composition suggesting isotopic exchange at equilibrium with a fluid of similar composition.

interpreted either as a result of melilite formation in an ^{16}O-poor gaseous reservoir or, more likely, as a result of preferential oxygen isotope exchange of melilite after (or during) formation of mineralogic zonation.

The properties of the Efremovka FG-CAIs studied here (small grain size and an overall mineralogic zonation produced by reheating without melting) make them useful for evaluating the formation of the internal isotopic variations in CV chondrite CAIs, and in particular for testing the solid-state diffusion exchange model. Because these CAIs appear not to have been melted, the models involving gas-melt exchange during dynamic crystallization do not apply.

High-Temperature Gas-Solid Oxygen Isotope Exchange

As noted earlier, the general lack of isotopic zoning in large (0.1–1 mm) crystals of melilite and anorthite in CG-CAIs appears to be inconsistent with the highly uniform ^{16}O-rich compositions of coexisting spinel and pyroxene if the mechanism involved high-temperature gas-solid isotope exchange (e.g., Ryerson and McKeegan 1994). However, because of the significant difference in grain size between the FG-CAIs and CG-CAIs, it is worthwhile to evaluate whether this mechanism can explain the oxygen isotope characteristics of the FG-CAIs from CV chondrites. To model oxygen self-diffusion in FG-CAIs, we assume that spinel, melilite, anorthite, and pyroxene in this CAI have similar grain sizes, ~5 μm in diameter, and were well-exposed to the nebular gas. We also assume that the maximum reheating temperature experienced by FG-CAIs was slightly below the melting temperature of diopside (1575 K). We modeled the simple case of a sphere in an infinite medium (Eq. 6-20 in Crank 1975):

$$M_t/M_\infty = 1 - 6/\pi^2 \times \sum_{n=1}^{\infty} [1/n^2 \times \exp(-Dn^2\pi^2 t/a^2)] \quad (1)$$

where D is diffusion coefficient, a is the radius of the sphere, t is the diffusion time, and M_t/M_∞ is the amount of matter diffusing in the sphere, for example, in this case, the isotopic exchange factor given as a proportion between the initial and final compositions. Diffusion coefficients and activation energies for dry (anhydrous) oxygen isotopic self-diffusion in anorthite, melilite, pyroxene, and spinel are taken from Ryerson and McKeegan (1994). The results of our calculations, illustrated in Fig. 9, indicate that by the time of essentially complete melilite equilibration (99% exchange reached in 7 hours), oxygen isotope exchange in spinel is negligible and that <6% of the oxygen in pyroxene is exchanged; this would correspond to a shift of only ~2.5‰ in Δ^{17}O, assuming that oxygen with a Δ^{17}O = 0‰ diffuses into

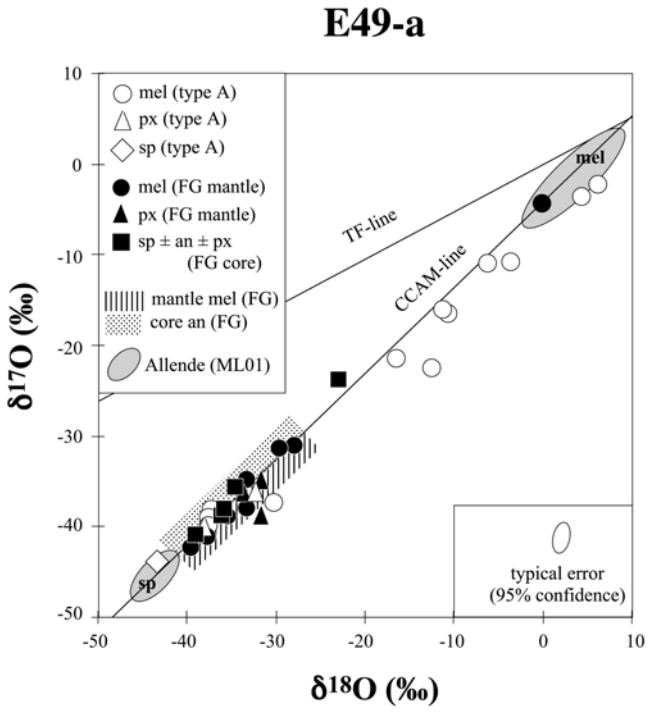

Fig. 8. Oxygen isotopic composition of the Efremovka CAI E49-a. Black symbols are for measurements in the fine-grained, spinel-rich inclusion (FG-E49-a); white symbols are for those in the coarse-grained, melilite-rich (type A) inclusion (TA-E49-a). Abbreviations are as used previously. Whereas FG-E49-a is consistently ^{16}O-rich (except two spots) and its composition lies on the CCAM line, the composition of melilite in TA-E49 is shifted to the right off the CCAM line as it is progressively depleted in ^{16}O.

an ^{16}O-rich solid with a $\Delta^{17}O = -25‰$. The exchange in anorthite is also small. However, for slightly longer heating times, on the order of a day or two, significant exchange does occur for anorthite, whereas pyroxene and spinel are still little affected. Such a scenario, which is generally consistent with postulated thermal histories for some CAIs, would result in intermediate compositions for anorthite similar to some of those inferred for the FG-CAIs examined here. Similar results were obtained for amoeboid olivine aggregate (AOA) minerals (spinel, pyroxene, anorthite, and olivine; Fagan et al. 2004a). Both sets of calculations show that oxygen diffusion theoretically fits with the observed isotopic patterns at the grain-to-grain scale in very fine grained objects. However, gas-solid diffusion would not generate larger scale zoning patterns similar to those observed in E42 and E67-1, for instance. It is thus necessary to evaluate the role of fluid-solid isotope exchange.

Low-Temperature Oxygen Isotope Exchange during Iron-Alkali Metasomatic Alteration

There exists some correlation between the degree of secondary alteration of the FG-CAIs from Efremovka and their oxygen isotopic compositions. For example, FG-E49-a, that shows rather uniform ^{16}O-enrichment, lacks nepheline and contains only iron-poor spinel (<0.4 wt% FeO; Table 2 in Krot et al. 2004). On the other hand, E67-1, which retains its original ^{16}O-enrichment only in spinel, contains relatively abundant nepheline and its spinel has variable iron contents (core: 0.17 wt% FeO; rim: 5.5 wt% FeO; Table 2 in Krot et al. 2004). E103a, which has an ^{16}O-enriched anorthite core and an ^{16}O-depleted melilite mantle, also contains traces of nepheline, but shows significant enrichment in FeO in spinel towards the periphery (core: 0.09 wt%; rim: 7.7 wt%; Table 2 in Krot et al. 2004).

This correlation is qualitatively similar to the situation that exists both in CAIs from metamorphosed CO chondrites which experienced iron-alkali metasomatic alteration that apparently modified oxygen isotopic compositions of CAIs (Wasson et al. 2001) and in AOAs from CV3 chondrites, which are also fine-grained, porous objects, which are highly sensitive to fluid circulations (Fagan et al. 2004a). This suggests that some of the oxygen isotope heterogeneity in the Efremovka FG-CAIs may have resulted from oxygen isotope exchange in the presence of a fluid phase, most likely in an asteroidal setting. However, the lack of experimental data on oxygen isotope exchange in the CAI minerals in the presence of an aqueous fluid does not permit quantification of the effects of alteration on their oxygen isotopic compositions.

It is interesting to note that no effects of aqueous alteration on oxygen isotopic composition of melilite were found in CAIs from CR chondrites (Aléon et al. 2002). Fine-grained, spinel-rich inclusions are found in these meteorites; the CR FG-CAIs are aggregates of spinel ± hibonite ± perovskite nodules surrounded by layers of melilite and Al-diopside, as they are in reduced CV chondrites. However, they do not show an overall macroscale mineralogic zonation and are uniformly ^{16}O-rich (Aléon et al. 2002). This suggests that, unlike the FG-CAIs in CV chondrites, those in CRs are pristine aggregates of condensates from an ^{16}O-rich gas that escaped both subsequent reheating and oxygen isotope exchange.

Compound CAI E49-a: Evidence for Oxygen Isotope Exchange in the Solar Nebula

The fine-grained, spinel-rich portion (FG-E49-a) and the coarse-grained, melilite-rich (TA-E49-a) portion of E49-a have different oxygen isotope compositions and different REE patterns (Huss et al. 2002), supporting the idea that this inclusion is a compound object (Krot et al. 2004). Oxygen isotopic compositions of spinel, pyroxene, and most of the anorthite and melilite grains in FG-E49-a are ^{16}O-rich ($\Delta^{17}O$ ~–20‰) and plot along the CCAM line. The group II REE pattern of FG-E49a (Huss et al. 2002) suggests that it condensed from an ^{16}O-rich gas depleted in ultrarefractory REE elements. TA-E49-a has both similarities and differences in its oxygen isotope composition to some of the coarse-grained type A CAIs in CV chondrites. As in coarse-grained

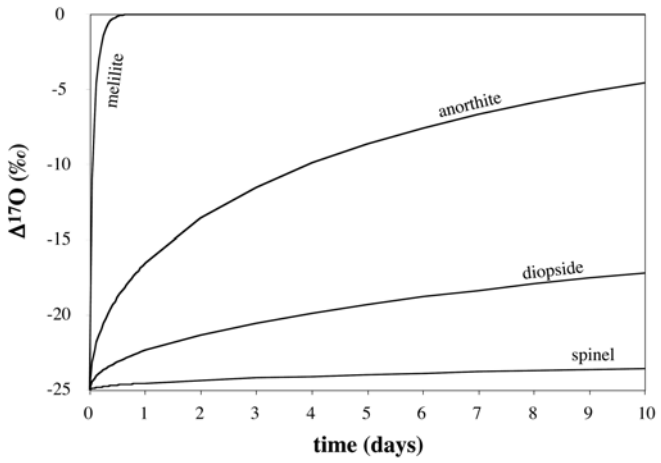

Fig. 9. Modeled oxygen isotopic compositions ($\Delta^{17}O$) of the initially, uniformly ^{16}O-rich ($\Delta^{17}O_{initial} = -25‰$) anorthite, diopside, melilite, and spinel grains, 5 μm in diameter, equilibrated with an ^{16}O-poor gas ($\Delta^{17}O = 0‰$) at 1575 K as a function of time. The intermineral oxygen isotopic compositions of the fine-grained, spinel-rich CAI E103a are generally consistent with the modeled solid-state oxygen self-diffusion.

type A CAIs, both spinel and pyroxene in TA-E49-a are uniformly ^{16}O-enriched (Fig. 8). However, melilite in TA-E49-a shows a large range of oxygen isotopic compositions ($\Delta^{17}O = -22‰$ up to $-6‰$), suggesting that this inclusion recorded partial oxygen isotope exchange. In contrast, melilite in most type A CAIs in CV chondrites experienced nearly complete equilibration with the surrounding reservoir and has uniformly ^{16}O-poor compositions. In addition, most of the analyses of melilite in TA-E49-a are shifted to the right off the CCAM line. Such a deviation is distinct from that observed in FUN inclusions, where it resulted from evaporation (e.g., Wasserburg et al. 1977; Lee et al. 1980; Davis et al. 1991, 2000). A similar shift off the CCAM line has been reported for melilite in a fluffy type A CAI from Vigarano by Harazono and Yurimoto (2003), who interpreted it as a result of interaction with an aqueous fluid in an asteroidal setting after oxygen isotope exchange. However, the fact that the finer-grained portion of E49-a is consistently ^{16}O-enriched compared to the coarse-grained type A portion is inconsistent with diffusion-controlled isotope exchange after the two parts joined together either in the solar nebula or on the CV asteroid: the opposite isotopic pattern would be expected. We conclude that the exchange must have occurred in the nebula prior to the formation of the compound object. This suggests that the shift to the right off the CCAM line could be attributed to a minor amount of mass fractionation occurring during the isotopic exchange, such as, for instance, evaporation during partial melting in a ^{16}O-poor reservoir.

Compound CAIs are rare objects: only four have been reported previously. El Goresy and Zinner (1994) described a compact type A (CTA) inclusion within another CTA. El Goresy et al. (2002) reported FG-CAI fragments within a CTA-CAI. Palisade bodies in two type B inclusions from Allende were proposed to be relict on the basis of their magnesium isotopic composition (Hsu et al. 2000) and of their oxygen isotopic composition (Kim et al. 2002), although palisade bodies are usually thought to form within the CAIs (Simon and Grossman 1997). The coexistence of isotopically distinct inclusions in the compound CAI E49-a suggests first that oxygen isotope exchange recorded by TA-E49-a occurred in the solar nebula, and also that TA-E49-a and FG-E49-a experienced different heating histories in the nebula, which implies that they formed in separate reservoirs and were transported before aggregation. The relative amount of heating undergone by the two parts still remains to be determined. Either TA-E49-a was heated to a stronger extent and experienced a more pronounced isotopic exchange, or TA-E49-a and FG-E49-a were heated in two different isotopic reservoirs. Given that the rim of the FG-E49-a is only partially preserved (Figs. 4d, 4, and 4g) and that the petrological limit is difficult to locate, it is likely that both inclusions were not completely cold when they aggregated. This implies that the inclusions were transported into nebular regions with different temperature regimes or different isotopic compositions in a short period of time, possibly days. If the latter suggestion is correct, then it implies that both ^{16}O-rich and ^{16}O-poor gaseous reservoirs existed simultaneously in the early solar nebula.

CONCLUSIONS

Three out of the four fine-grained, spinel-rich CAIs we studied in Efremovka show variations in their oxygen isotopic composition: spinel is uniformly ^{16}O-enriched ($\Delta^{17}O$ ~−20‰), pyroxene is mostly ^{16}O-rich, although more variable than spinel, and anorthite and melilite are highly variable within individual inclusions and range in composition from ^{16}O-rich ($\Delta^{17}O$ ~−20‰) to ^{16}O-poor ($\Delta^{17}O$ ~−5‰), unlike in coarse-grained, igneous CAIs from CV chondrites that generally have uniformly ^{16}O-depleted melilite. Also, the degrees of ^{16}O-depletion of melilite and anorthite in FG-CAIs are smaller than those in the same phases in CG-CAIs from CV chondrites. Spinel, pyroxene, and even most melilite and anorthite grains in the fine-grained, spinel-rich portion of a compound CAI E49-a are ^{16}O-enriched ($\Delta^{17}O$ ~−20‰), whereas melilite in the coarse-grained, melilite-rich (type A) portion of this same CAI shows a large range in oxygen isotopic compositions ($\Delta^{17}O = -22‰$ up to $-6‰$) that are systematically shifted to the right off the CCAM line.

We infer that the fine-grained, spinel-rich CAIs from Efremovka formed by aggregation of gas-solid condensates from an ^{16}O-rich gaseous reservoir. They subsequently experienced reheating in the same gaseous reservoir, followed by reprocessing in an ^{16}O-poor gaseous reservoir that resulted in various degrees of oxygen isotope exchange. In general, the patterns and degrees of isotopic exchange within mineral phases of FG-CAIs are consistent with gas-solid diffusion.

However, isotopic macrozoning in some Efremovka FG-CAIs and correlated volatile element abundances and ^{16}O depletions in others suggest that, in at least some cases, the oxygen isotope distributions were further modified by minor secondary mineralogic alteration, possibly in a late-stage parent body event.

The presence of a compound CAI composed of a fine-grained, spinel-rich inclusion with a type A inclusion having different oxygen isotope systematics suggests that oxygen isotope exchange in the type A CAI occurred in the solar nebula prior to the formation of the compound object. The observed isotopic compositions of this compound object are best understood if ^{16}O-rich and ^{16}O-poor gaseous reservoirs existed simultaneously in different locales in the solar nebula and implies radial transport of still-hot CAIs, possibly over large scales in the solar nebula.

Acknowledgments–We are grateful to Gary Huss for providing unpublished REE data of the Efremovka CAIs studied. George Jarzebinski and Chris Coath helped care for the UCLA ion microprobe. Discussions with Sara Russell and Ahmed El Goresy were useful and are highly appreciated. Stéphanie Duchène is thanked for discussions regarding diffusion calculations. We thank H. Yurimoto and an anonymous reviewer for constructive reviews, and E. Zinner for careful editorial work. This work was supported by NASA grants NAG5-4704 (K. D. McKeegan, P.I.), NAG5-13131 (A. N. Krot, P.I.), NAG5-10468 (G. J. MacPherson, P.I.), and NAG5-11591 (K. Keil, P.I.). The UCLA Ion Microprobe Laboratory is partially supported by a grant from the NSF Instrumentation and Facilities program. This is Hawai'i Institute of Geophysics and Planetology publication No. 1405 and School of Ocean and Earth Science and Technology publication No. 6651. This is CRPG CNRS contribution No. 1748.

Editorial Handling—Dr. Ernst Zinner

REFERENCES

Aléon J., Krot A. N., and McKeegan K. D. 2002. Ca-Al-rich inclusions and amoeboid olivine aggregates from the CR carbonaceous chondrites. *Meteoritics & Planetary Science* 37: 1729–1755.

Boynton W. V. 1975. Fractionation in the solar nebula—Condensation of yttrium and the rare earth elements. *Geochimica et Cosmochimica Acta* 39:569–584.

Brigham C. A., Papanastassiou D. A., and Wasserburg G. J. 1985. Mg isotopic heterogeneities in fine-grained Ca-Al-rich inclusions (abstract). Proceedings, 16th Lunar and Planetary Science Conference. pp. 93–94.

Clayton R. N. 1993. Oxygen isotopes in meteorites. *Annual Review of Earth and Planetary Sciences* 21:115–149.

Clayton R. N. 2002. Self-shielding in the solar nebula. *Nature* 415: 860–861.

Clayton R. N. and Mayeda T. K. 1984. The oxygen isotope record in Murchison and other carbonaceous chondrites. *Earth and Planetary Science Letters* 67:151–161.

Clayton R. N., Onuma N., Grossman L., and Mayeda T. K. 1977. Distribution of the presolar component in Allende and other carbonaceous chondrites. *Earth and Planetary Science Letters* 34:209–224.

Crank J. 1975. *The mathematics of diffusion.* 2nd ed. Oxford, UK: Oxford University Press. 414 p.

Davis A. M. and Grossman L. 1979. Condensation and fractionation of rare earths in the solar nebula. *Geochimica et Cosmochimica Acta* 43:1611–1632.

Davis A. M. and Richter F. M. 2004. Elemental and isotopic fractionation by diffusion-limited evaporation (abstract #2047). 35th Lunar and Planetary Science Conference. CD-ROM.

Davis A. M., MacPherson G. J., Clayton R. N., Mayeda T. K., Sylvester P. J., Grossman L., Hinton R. W., and Laughlin J. R. 1991. Melt solidification and late-stage evaporation in the evolution of a FUN inclusion from the Vigarano C3V chondrite. *Geochimica et Cosmochimica Acta* 55:621–637.

Davis A. M., McKeegan K. D., and MacPherson G. J. 2000. Oxygen-isotopic compositions of individual minerals from the FUN inclusion Vigarano 1623-5 (abstract). *Meteoritics & Planetary Science* 35:A47.

El Goresy A. and Zinner E. K. 1994. Efremovka E49: A compact type A CAI containing a partially molten spinel-melilite-diopside xenolith (abstract). *Meteoritics* 29:461–462.

El Goresy A., Zinner E., Matsunami S., Palme H., Spettel B., Lin Y. and Nazarov M. 2002. Efremovka 101.1: A CAI with ultrarefractory REE patterns and enormous enrichments of Sc, Zr, and Y in fassaite and perovskite. *Geochimica et Cosmochimica Acta* 66:1459–1491.

Esat T. M. and Taylor S. R. 1984. FREE FUN with Mg in Allende group II inclusions (abstract). Proceedings, 15th Lunar and Planetary Science Conference. pp. 254–255.

Fagan T. J., McKeegan K. D., Krot A. N., and Keil K. 2001. Calcium-aluminum-rich inclusions in enstatite chondrites (II): Oxygen isotopes. *Meteoritics & Planetary Science* 36:223–230.

Fagan T. J., Krot A. N., Keil K., and Yurimoto H. 2004a. Oxygen isotopic evolution of amoeboid olivine aggregates in the reduced CV3 chondrites Efremovka, Vigarano, and Leoville. *Geochimica et Cosmochimica Acta* 68:2591–2611.

Fagan T. J., Krot A. N., Keil K. and Yurimoto H. 2004b. Oxygen isotopic alteration in Ca-Al-rich inclusions from Efremovka: Nebular or parent-body setting? *Meteoritics & Planetary Science* 39:1257–1272.

Greenwood J. P. 2004. Disequilibrium melting of refractory inclusions: A mechanism for high-temperature oxygen isotope exchange in the solar nebula (abstract #2132). 35th Lunar and Planetary Science Conference. CD-ROM.

Grossman L. and Ganapathy R. 1976. Trace elements in the Allende meteorite—II. Fine-grained, Ca-rich inclusions. *Geochimica et Cosmochimica Acta* 40:967–977.

Guan Y., McKeegan K. D., and MacPherson G. J. 2000. Oxygen isotopes in calcium-aluminum-rich inclusions from enstatite chondrites: New evidence for a single CAI source in the solar nebula. *Earth and Planetary Science Letters* 181:271–277.

Harazono K. and Yurimoto H. 2003. Oxygen isotopic variations in a fluffy type A CAI from the Vigarano meteorite (abstract #1540). 34th Lunar and Planetary Science Conference. CD-ROM.

Hiyagon H. and Hashimoto A. 1999. ^{16}O excesses in olivine inclusions in Yamato-86009 and Murchison chondrites and their relation to CAIs. *Science* 283:828–831.

Hsu W., Wasserburg G. J., and Huss G. R. 2000. High time resolution by use of the ^{26}Al chronometer in the multistage formation of a CAI. *Earth and Planetary Science Letters* 182:15–29.

Huss G. R., MacPherson G. J., Davis A. M., Krot A. N., and Ulyanov A. A. 2002. Microdistribution of REE in fine-grained group II CAIs in Efremovka (abstract). *Meteoritics & Planetary Science* 37:A68.

Ito M., Nagasawa H., and Yurimoto H. 2004. Oxygen isotopic SIMS analysis in Allende CAI: Details of the very early thermal history of the solar system. *Geochimica et Cosmochimica Acta* 68:2905–2923.

Itoh S., Kojima H., and Yurimoto H. 2004. Petrography and oxygen isotopic compositions in refractory inclusions from CO chondrites. *Geochimica et Cosmochimica Acta* 68:183–194.

Kim G. L., Yurimoto H., and Sueno S. 2002. Oxygen isotopic composition of a compound Ca-Al-rich inclusion from Allende meteorite: Implication for origin of palisade bodies and O-isotopic environment in the CAI forming region. *Journal of Mineralogical and Petrological Sciences* 97:161–167.

Krot A. N., McKeegan K. D., Russell S. S., Meibom A., Weisberg M. K., Zipfel J., Krot T. V., Fagan T. J., and Keil K. 2001. Refractory calcium-aluminum-rich inclusions and aluminum-diopside-rich chondrules in the metal-rich chondrites Hammadah al Hamra 237 and Queen Alexandra Range 94411. *Meteoritics & Planetary Science* 36:1189–1216.

Krot A. N., McKeegan K. D., Leshin L. A., MacPherson G. J., and Scott E. R. D. 2002. Existence of an ^{16}O-rich gaseous reservoir in the solar nebula. *Science* 295:1051–1054.

Krot A. N., MacPherson G. J., Ulyanov A. A., and Petaev M. I. 2004. Fine-grained, spinel-rich inclusions from the reduced CV chondrites Efremovka and Leoville: I. Mineralogy, petrology, and bulk chemistry. *Meteoritics & Planetary Science* 39:1517–1553.

Lee T., Mayeda T. K., and Clayton R. N. 1980. Oxygen isotopic anomalies in Allende inclusion HAL. *Geophysical Research Letters* 7:493–496.

Lyons J. R. and Young E. D. 2005. CO self-shielding as the origin of oxygen isotope anomalies in the early solar nebula. *Nature* 435: 317–320.

MacPherson G. J., Krot A. N., Ulyanov A. A., and Hicks T. 2002. A comprehensive study of pristine, fine-grained, spinel-rich inclusions from the Leoville and Efremovka CV3 Chondrites, I: Petrology (abstract #1526). 33rd Lunar and Planetary Science Conference. CD-ROM.

Marcus R. A. 2004. Mass-independent isotope effect in the earliest processed solids in the solar system: A possible chemical mechanism. *Journal of Chemical Physics* 121:8201–8211.

McGuire A. V. and Hashimoto A. 1989. Origin of zoned fine-grained inclusions in the Allende meteorite. *Geochimica et Cosmochimica Acta* 53:1123–1133.

McKeegan K. D. and Leshin L. A. 2001. Stable isotope variations in extraterrestrial materials. In *Stable isotope geochemistry*, edited by Valley J. W. and Cole D. R. Washington, D.C.: Mineralogical Society of America. pp. 279–378.

McKeegan K. D., Leshin L. A., Russell S. S., and MacPherson G. J. 1998. Oxygen isotopic abundances in calcium-aluminum-rich inclusions from ordinary chondrites: Implications for nebular heterogeneity. *Science* 280:414–417.

Robert F. 2003. The common property of isotopic anomalies in meteorites. *Astronomy and Astrophysics* 415:1167–1176.

Ryerson F. J. and McKeegan K. D. 1994. Determination of oxygen self-diffusion in åkermanite, anorthite, diopside, and spinel; Implications for oxygen isotopic anomalies and the thermal histories of Ca-Al-rich inclusions. *Geochimica et Cosmochimica Acta* 58:3713–3734.

Sahijpal S., McKeegan K. D., Krot A. N., Weber D., and Ulyanov A. A. 1999. Oxygen isotopic compositions of Ca-Al-rich inclusions from the CH chondrites, Acfer 182 and PAT 91546 (abstract). *Meteoritics & Planetary Science* 34:A101.

Scott E. R. D. and Krot A. N. 2001. Oxygen isotopic compositions and origins of calcium-aluminum-rich inclusions and chondrules. *Meteoritics & Planetary Science* 36:1307–1319.

Simon S. B. and Grossman L. 1997. In situ formation of palisade bodies in calcium, aluminum-rich inclusions. *Meteoritics & Planetary Science* 32:61–70.

Stolper E. M. 1982. Crystallization sequences of Ca-Al-rich inclusions from Allende; an experimental study. *Geochimica et Cosmochimica Acta* 46:2159–2180.

Tanaka T. and Masuda A. 1973. Rare-earth elements in matrix, inclusions, and chondrules of the Allende meteorite. *Icarus* 19: 523–530.

Thiemens M. H. and Heidenreich J. E. 1983. The mass-independent fractionation of oxygen: A novel isotope effect and its possible cosmochemical implications. *Science* 219:1073–1075.

Ulyanov A. A. 1984. On the origin of fine-grained Ca, Al-rich inclusions in the Efremovka carbonaceous chondrite (abstract). Proceedings, 35th Lunar & Planetary Science Conference. pp. 872–873.

Wark D. A. 1981. The pre-alteration compositions of Allende Ca-Al-rich inclusions (abstract). Proceedings, 12th Lunar and Planetary Science Conference. pp. 1148–1150.

Wark D. A. and Lovering J. F. 1977. Marker events in the early solar system: Evidence from rims on Ca-Al-rich inclusions in carbonaceous chondrites. Proceedings, 8th Lunar and Planetary Science Conference. pp. 95–112.

Wark D. A., Kornacki A. S., Boynton W. V., and Ulyanov A. A. 1986. Efremovka fine-grained inclusion E14: Comparisons with Allende (abstract). Proceedings, 12th Lunar and Planetary Science Conference. pp. 921–922.

Wasserburg G. J., Lee T., and Papanastassiou D. A. 1977. Correlated O and Mg isotopic anomalies in Allende inclusions. II—Magnesium. *Geophysical Research Letters* 4:299–302.

Wasson J. T., Yurimoto H., and Russell S. S. 2001. ^{16}O-rich melilite in CO3 chondrites: Possible formation of common ^{16}O-poor melilite by aqueous alteration. *Geochimica et Cosmochimica Acta* 65:4539–4549.

Young E. D. and Russell S. S. 1998. Oxygen reservoirs in the early solar nebula inferred from an Allende CAI. *Science* 282:452–455.

Young E. D., Ash R. D., England P., and Rumble D. 1999. Fluid flow in chondritic parent bodies: Deciphering the compositions of planetesimals. *Science* 286:1331–1335.

Yurimoto H. and Kuramoto K. 2004. Molecular cloud origin for the oxygen isotope heterogeneity in the solar system. *Science* 305: 1763–1766.

Yurimoto H., Morioka M., and Nagasawa H. 1989. Diffusion in single crystals of melilite. I—Oxygen. *Geochimica et Cosmochimica Acta* 53:2387–2394.

Yurimoto H., Ito M., and Nagasawa H. 1998. Oxygen isotope exchange between refractory inclusion in Allende and solar nebula gas. *Science* 282:1874–1877.